ON THE RECONSTRUCTION PROBLEM FOR PASCAL LINES

Abdelmalek Abdesselam and Jaydeep Chipalkatti

ABSTRACT: Given a sextuple of distinct points A, B, C, D, E, F on a conic, arranged into an array $\begin{bmatrix} A & B & C \\ F & E & D \end{bmatrix}$, Pascal's theorem says that the points $AE \cap BF, BD \cap CE, AD \cap CF$ are collinear. The line containing them is called the Pascal of the array, and one gets altogether sixty such lines by permuting the points. In this paper we prove that the initial sextuple can be explicitly reconstructed from four specifically chosen Pascals. The reconstruction formulae are encoded by some transvectant identities which are proved using the graphical calculus for binary forms.

AMS subject classification (2010): 14N05, 22E70, 51N35.

Keywords: Pascal lines, transvectants, invariant theory of binary forms.

1. INTRODUCTION

This paper solves a reconstruction problem which arises in the context of Pascal's hexagram in classical projective geometry. The main result will be explained below once the required notation is available.

1.1. Let $\mathbf{P}^2$ denote the complex projective plane, and fix a nonsingular conic $\mathcal{K}$ in $\mathbf{P}^2$. Suppose that we are given six distinct points A, B, C, D, E, F on $\mathcal{K}$, arranged as an array $\begin{bmatrix} A & B & C \\ F & E & D \end{bmatrix}$. Then Pascal's theorem[1] says that the three cross-hair intersection points

$$AE \cap BF, \quad BD \cap CE, \quad AD \cap CF$$

(corresponding to the three minors of the array) are collinear.

The line containing them is called the Pascal line, or just the Pascal, of the array; we will denote it by $\left\{ \begin{matrix} A & B & C \\ F & E & D \end{matrix} \right\}$. It is easy to see that the Pascal remains unchanged if we

[1] One can find a proof in virtually any book on elementary projective geometry, e.g., Pedoe [21, Ch. IX] or Seidenberg [25, Ch. 6]. It is doubtful whether Pascal himself had a proof.

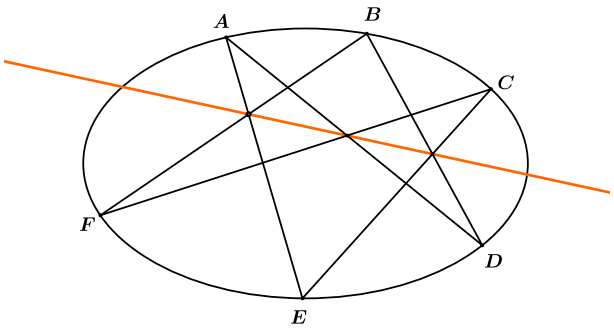

DIAGRAM 1. Pascal's theorem

permute the rows or the columns of the array; thus

$$\left\{\begin{array}{ccc} A & B & C \\ F & E & D \end{array}\right\}, \quad \left\{\begin{array}{ccc} F & E & D \\ A & B & C \end{array}\right\}, \quad \left\{\begin{array}{ccc} E & D & F \\ B & C & A \end{array}\right\} \tag{1.1}$$

all denote the same line. Any essentially different arrangement of the same points, say $\left\{\begin{array}{ccc} E & A & C \\ B & F & D \end{array}\right\}$, corresponds *a priori* to a different line. Hence we have a total of $\frac{6!}{2!3!} = 60$ notionally distinct Pascals. It is a theorem due to Pedoe [20], that these 60 lines are distinct if the initial six points are chosen generally.[2] The configuration of six points with all of its associated lines is sometimes called Pascal's hexagram. The best classical references for the geometry of Pascal lines are by Salmon [23, Notes] and Baker [3, Note II, pp. 219–236]. An engaging recent account is given in the article by Conway and Ryba [8]. The reader is referred to [15] and [25] for standard facts about projective planes.

1.2. It is natural to wonder to what extent the construction sequence

$$\text{six points on } \mathcal{K} \rightsquigarrow \text{sixty lines in the plane}$$

can be reversed; that is to say, whether one can *reconstruct* the initial sextuple if the positions of some of the Pascals are known.[3] In this paper we establish the following result:

The Main Theorem (Preliminary Form)**.** The sextuple $A, \ldots, F$ can be reconstructed from the following four Pascals:

$$\ell_1 = \left\{\begin{array}{ccc} A & D & B \\ E & C & F \end{array}\right\}, \quad \ell_2 = \left\{\begin{array}{ccc} A & C & F \\ E & D & B \end{array}\right\}, \quad \ell_3 = \left\{\begin{array}{ccc} A & D & F \\ E & C & B \end{array}\right\}, \quad \ell_\star = \left\{\begin{array}{ccc} A & B & C \\ F & D & E \end{array}\right\}. \tag{1.2}$$

[2] If one tries to draw a diagram of the sextuple together with all sixty of its Pascals, a dense and incomprehensible profusion of ink is the usual outcome. The curious reader is referred to `http://mathworld.wolfram.com/PascalLines.html`

[3] The conic itself is fixed throughout, and as such assumed to be known.

The arrays follow a pattern and the last one is on a different footing from the first three; this will be explained in section 1.4.

1.3. In order to state the theorem more precisely, let $[z_0, z_1, z_2]$ be the homogeneous coordinates on $\mathbf{P}^2$, and let the conic $\mathcal{K}$ be defined by the equation $z_1^2 = z_0\, z_2$. Lines in $\mathbf{P}^2$ are also given by homogeneous coordinates; for instance, the line $2\,z_0 + 3\,z_1 + 5\,z_2 = 0$ has line coordinates $\langle 2, 3, 5\rangle$. Choose independent variables $a, \ldots, f$, and fix the points

$$A = [1, a, a^2], \quad B = [1, b, b^2], \quad \ldots, F = [1, f, f^2] \tag{1.3}$$

on $\mathcal{K}$. Let $\langle 1, s_i, t_i\rangle$ denote the line coordinates of ℓ_i for $i = 1, 2, 3$, and $\langle 1, s_*, t_*\rangle$ those of ℓ_*. Each of these Pascals is obtained by starting from the points in (1.3) and taking joins and intersections, hence it is intuitively clear that s_i and t_i are rational functions in $a, \ldots, f$. The actual expressions are rather cumbersome; for instance,

$$s_1 = \frac{abf - abe - acd + 9 \text{ similar terms}}{abce - abcf + 4 \text{ similar terms}}, \quad t_1 = \frac{ac - af - bc + 3 \text{ similar terms}}{abce - abcf + 4 \text{ similar terms}}, \tag{1.4}$$

and likewise for the other s_i, t_i. The reconstruction problem is to go backwards from the collection of Pascals $\{\ell_1, \ell_2, \ell_3, \ell_*\}$ to the collection of points $\{A, \ldots, F\}$. Our result says that this can be done in algebraically the simplest possible way.

The Main Theorem (Refined Form)**.** Each of the variables $a, \ldots, f$ can be expressed as a rational function of s_i and t_i for $i = 1, 2, 3, *$.

A naive attempt to prove the theorem would start from the formulae for $s_1, \ldots, t_*$, and try to 'solve' for the variables $a, \ldots, f$. However, the expressions in (1.4) are too complicated for this to succeed. We will instead use binary quadratic forms to represent points and lines in $\mathbf{P}^2$, and express their joins and intersections in the language of transvectants (see section 2). One can then make these rational functions completely explicit by exploiting the geometry of the Pascals in conjunction with the graphical calculus for binary forms. It is an immediate corollary of the main theorem that the Galois group of Pascal lines is isomorphic to the symmetric group $\mathfrak{S}_6$. Our main theorem is thematically similar to, and partly inspired by, Wernick's problems in Euclidean triangle geometry [24, 26].

1.4. An overview of the proof. The relevant geometric elements are shown in Diagram 2 on page 5. Since each Pascal corresponds to a 2×3 array (determined up to a shuffling of rows and columns), its columns give a partition of the points $A, \ldots, F$ into three sets of two elements each. For instance, any of the arrays in (1.1) gives the partition

$$\{A, F\} \cup \{B, E\} \cup \{C, D\}.$$

Now observe that the first three Pascals in (1.2) have been so chosen that they all lead to the same partition, namely

$$\{A, E\} \cup \{C, D\} \cup \{B, F\}. \tag{1.5}$$

This corresponds to the three green chords in Diagram 2. Let Q_1 denote the point $AB \cap EF$, which is common to ℓ_2 and ℓ_3. Similarly, let

$$Q_2 = \ell_3 \cap \ell_1 = AC \cap DE, \qquad Q_3 = \ell_1 \cap \ell_2 = BC \cap DF. \tag{1.6}$$

Hence the line Q_1Q_2 is the same as ℓ_3, and so on. Now, if we switch the endpoints of all the three chords simultaneously; that is to say, if we apply the product of transpositions $(A\,E)\,(C\,D)\,(B\,F)$, then all the Q_i remain unchanged and hence so do the first three Pascals. In other words, each of the expressions $s_1, t_1, \ldots, s_3, t_3$ remains invariant if we make a simultaneous substitution of variables $a \leftrightarrow e, c \leftrightarrow d, b \leftrightarrow f$. It follows that no rational function of $s_1, \ldots, t_3$ can equal any of the variables $a, \ldots, f$.

The **first stage** in the proof is to show that the next best outcome is achievable; that is to say, the symmetric expressions

$$a + e, \quad a\,e, \quad b + f, \quad b\,f, \quad c + d, \quad c\,d$$

are rational functions of $s_1, \ldots, t_3$. In geometric terms (see the top part of Diagram 2), the red triangle $Q_1Q_2Q_3$ allows us to locate the three green chords, but we do not yet have sufficient information to label their endpoints. The algebraic formulae which connect the red triangle to the green chords are encoded in a transvectant identity.

In the **second stage**, we bring in the fourth Pascal ℓ_* (shown in blue) to break the symmetry. It is so chosen that each of the three green chords passes through one of the cross-hair intersections in ℓ_*; for instance, BF passes through the point $AD \cap BF$ on ℓ_*. And now, another transvectant identity allows us to get a linear equation for a whose coefficients are rational functions in $s_1, \ldots, t_*$. This implies that a itself is such a function, and a similar argument applies to $b, \ldots, f$. This gives the required result.

2. BINARY FORMS

2.1. Let $\mathcal{E}$ denote the field $\mathbf{Q}(a, b, c, d, e, f)$ of rational functions in the variables $a, \ldots, f$. We will use $\mathcal{E}$ as our base field, so that any 'scalar' will be assumed to belong to $\mathcal{E}$. Henceforth, the projective plane $\mathbf{P}^2$ will be over $\mathcal{E}$. We will consider homogeneous forms in the variables $\mathbf{x} = (x_1, x_2)$. In a classical notation introduced by Cayley, $(z_0, z_1, \ldots, z_n)(x_1, x_2)^n$ stands for the degree n form $\sum_{i=0}^{n} z_i \binom{n}{i} x_1^{n-i} x_2^i$.

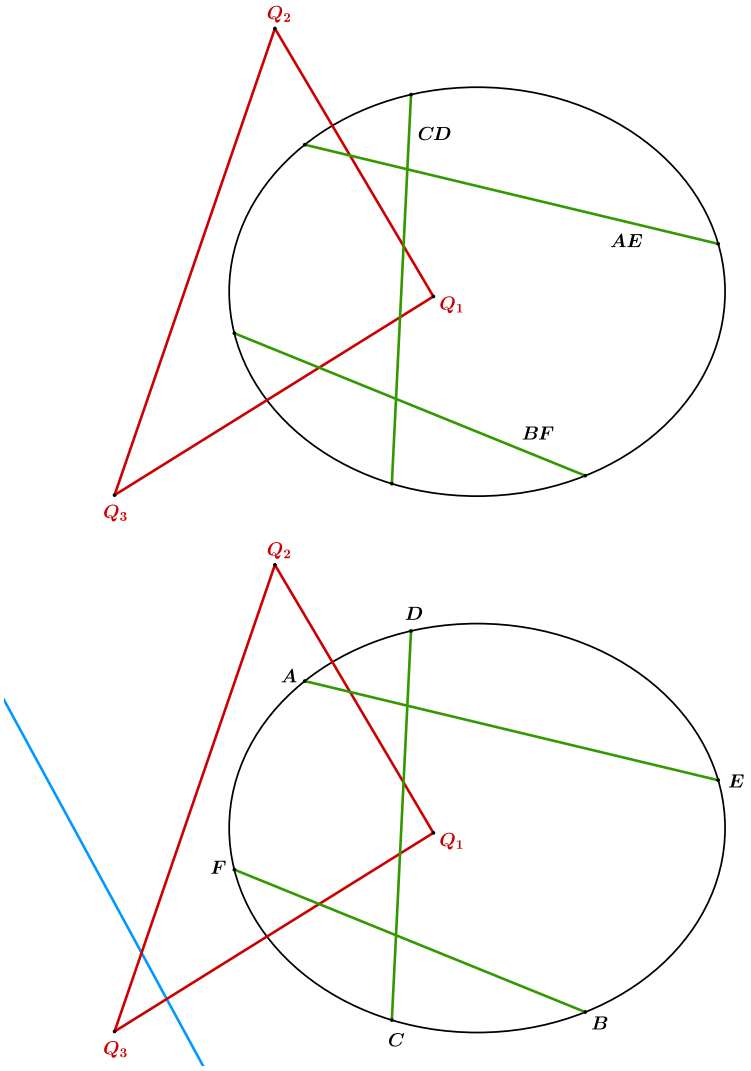

DIAGRAM 2. *Dramatis Personae* in the reconstruction

2.2. Transvectants. Although the definition of a transvectant is *prima facie* technical, the concept arises naturally in invariant theory and representation theory (see [19, Ch. 5]). Suppose that we are given two binary forms G, H of degrees m, n respectively. For an integer $r \geqslant 0$, their r-th transvectant is defined to be

$$(G, H)_r = \frac{(m-r)!\,(n-r)!}{m!\,n!} \sum_{i=0}^{r} (-1)^i \binom{r}{i} \frac{\partial^r G}{\partial x_1^{r-i}\,\partial x_2^i} \frac{\partial^r H}{\partial x_1^i\,\partial x_2^{r-i}} \tag{2.1}$$

This is a form of degree $m + n - 2r$, unless it is identically zero. If

$$G = (g_0, g_1, g_2 \rangle\!\rangle x_1, x_2)^2, \quad H = (h_0, h_1, h_2 \rangle\!\rangle x_1, x_2)^2,$$

then it is easy to check that

$$(G,H)_1 = (g_0h_1 - g_1h_0, \frac{1}{2}(g_0\,h_2 - g_2\,h_0), g_1\,h_2 - g_2\,h_1)(x_1,x_2)^2, \text{ and}$$
$$(G,H)_2 = g_0h_2 - 2\,g_1h_1 + g_2h_0.$$

In general, the coefficients of $(G,H)_r$ are linear functions in the coefficients of G and H. The numerical factors in Cayley's notation and (2.1) may seem unnecessary, but experience has shown that they simplify the computations.

2.3. Now the crucial step is to represent points and lines in $\mathbf{P}^2$ by quadratic binary forms. (The reader may also refer to [6, §3] where an identical set-up is used.) Let the nonzero quadratic form $G = (g_0, g_1, g_2)(x_1, x_2)^2$ represent the point $P_G = [g_0, g_1, g_2]$, as well as the line $L_G = \langle g_2, -2\,g_1, g_0\rangle$. It is understood that any nonzero scalar multiple of G will represent the same point or line. Now the following properties show that incidences and joins are exactly mirrored by transvectants.

Lemma 2.1. With notation as above,

(1) The point P_G belongs to the line L_H, if and only if $(G,H)_2 = 0$.
(2) The line joining the points P_G and P_H is $L_{(G,H)_1}$.
(3) The point of intersection of the lines L_G and L_H is $P_{(G,H)_1}$.

All the proofs follow immediately from the definitions. The point $P_G = [g_0, g_1, g_2]$ lies on $L_H = \langle h_2, -2\,h_1, h_0\rangle$ exactly when the dot product of the two vectors is zero, which proves (1). The equation of the line joining P_G and P_H is $\begin{vmatrix} z_0 & z_1 & z_2 \\ g_0 & g_1 & g_2 \\ h_0 & h_1 & h_2 \end{vmatrix} = 0$, hence it is represented by $(G,H)_1$. The proof of (3) is similar. □

The following result will be needed later.

Lemma 2.2. Two nonzero quadratic forms G and H are equal up to a scalar, if and only if $(G,H)_1 = 0$.

Proof. The forms are equal up to a scalar exactly when the matrix $\begin{bmatrix} g_0 & g_1 & g_2 \\ h_0 & h_1 & h_2 \end{bmatrix}$ has rank one, i.e., exactly when all of its minors are zero. This is equivalent to the vanishing of all the coefficients of $(G,H)_1$. □

The advantage of using transvectants is that there are well-developed tools for manipulating them, namely, a symbolic calculus (see [11, 19]) as well as a graphical calculus (see [1,

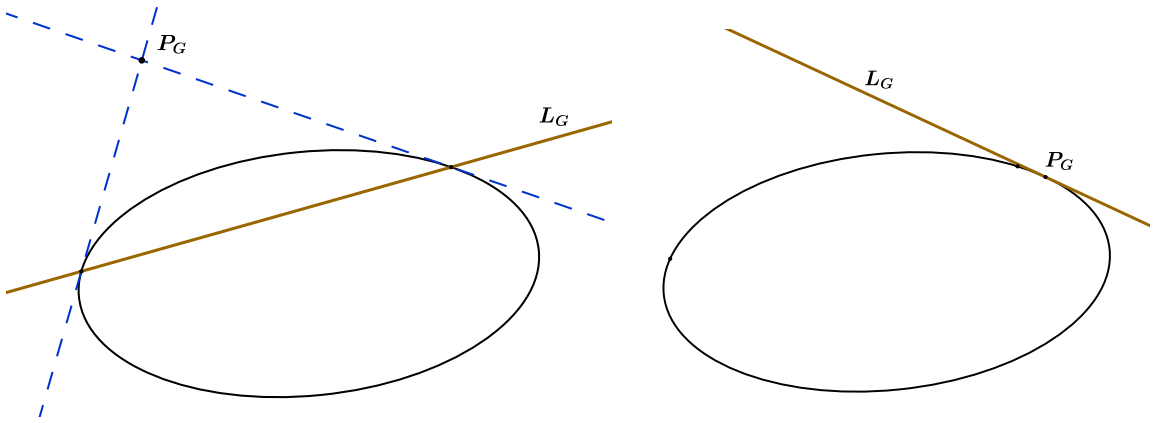

DIAGRAM 3. The pole-polar relation

§2]). This is especially useful when one encounters transvectants whose components are themselves transvectants.

2.4. The conic $\mathcal{K}$ consists of those points P_G such that

$$(G, G)_2 = 2\,(g_1^2 - g_0\,g_2) = 0.$$

These are the nonzero forms G which can be written as squares of linear forms up to a scalar. Define six linear forms

$$a_{\mathbf{x}} = x_1 + a\,x_2, \quad b_{\mathbf{x}} = x_1 + b\,x_2, \quad \dots \quad f_{\mathbf{x}} = x_1 + f\,x_2,$$

and fix the points $A = P_{a_{\mathbf{x}}^2}, \dots, F = P_{f_{\mathbf{x}}^2}$ on $\mathcal{K}$. Let

$$\lambda_i = (t_i, -\frac{s_i}{2}, 1)(x_1, x_2)^2, \qquad i = 1, 2, 3, *\tag{2.2}$$

denote the quadratic forms which represent the Pascals ℓ_i. All of this agrees with the notational conventions in section 1.3. The following lemma is helpful in completing the geometric picture, but it will not be needed elsewhere (see Diagram 3).

Lemma 2.3. Let G denote a nonzero quadratic form. Then L_G is the polar line of P_G with respect to $\mathcal{K}$. In particular,

$$P_G \text{ lies on } L_G \iff P_G \text{ lies on } \mathcal{K} \iff L_G \text{ is tangent to } \mathcal{K}.$$

The proof is left to the reader.

2.5. For instance, the line AB is represented by the form $(a_{\mathbf{x}}^2, b_{\mathbf{x}}^2)_1 = (b - a)\,a_{\mathbf{x}}\,b_{\mathbf{x}}$, or after ignoring the scalar, just by $a_{\mathbf{x}}\,b_{\mathbf{x}}$. It follows that the points Q_1, Q_2, Q_3 in section 1.4 are respectively represented by the quadratic forms

$$\pi_1 = (a_{\mathbf{x}}b_{\mathbf{x}}, e_{\mathbf{x}}f_{\mathbf{x}})_1, \quad \pi_2 = (a_{\mathbf{x}}c_{\mathbf{x}}, d_{\mathbf{x}}e_{\mathbf{x}})_1, \quad \pi_3 = (b_{\mathbf{x}}c_{\mathbf{x}}, d_{\mathbf{x}}f_{\mathbf{x}})_1.\tag{2.3}$$

Since $Q_1 = \ell_2 \cap \ell_3$ etc, they are also respectively represented by

$$\mu_1 = (\lambda_2, \lambda_3)_1, \quad \mu_2 = (\lambda_3, \lambda_1)_1, \quad \mu_3 = (\lambda_1, \lambda_2)_1. \tag{2.4}$$

This implies that μ_i and π_i are equal up to a multiplicative scalar in $\mathcal{E}$. It is clear that the coefficients of μ_i are rational functions in $s_1, \ldots, t_3$.

3. The proof of the main theorem

3.1. The first stage. For any quadratic forms U, V, W, define

$$\psi(U, V, W) = 6\,(U, VW)_2 - U(V, W)_2,$$

which is also a quadratic form.

Proposition 3.1. We have an identity

$$\psi(\pi_3, \pi_1, \pi_2) = \Phi \times a_{\mathbf{x}}\, e_{\mathbf{x}}, \tag{3.1}$$

where Φ is a polynomial in $a, \ldots, f$.

The proof will be given in section 4 using the graphical calculus, but the rationale behind the proposition can be explained without it. The right-hand side of (3.1) represents the line AE. Since μ_i is proportional to π_i, the left-hand side is proportional to $\psi(\mu_3, \mu_1, \mu_2)$. Hence the identity implies that AE can be represented by a form

$$\lambda_{AE} = (\alpha_{AE}, \beta_{AE}, 1)(x_1, x_2)^2,$$

where α_{AE}, β_{AE} are rational functions of $s_1, \ldots, t_3$. We can similarly write down λ_{CD} and λ_{BF} representing the other two green chords in Diagram 2. The exact expression for Φ will be found in the course of proving the identity, but it is immaterial to the main theorem.

Formula (3.1) was initially obtained by some calculated guesswork guided by intuition. Since the construction of Pascals is synthetic, if it is at all possible to pass from the red triangle to the green chords, then the connecting formula can be plausibly written in terms of transvectants. Since the letters a, e enter symmetrically into the expressions for π_1, π_2, the formula should respect this structure as well. Now the correct definition of ψ is determined by a graphical calculation, in which the initial intuition is buttressed by a formal proof. A direct calculation shows that

$$\alpha_{AE} = \frac{s_1^2\, s_3\, t_2\, t_3 - s_1^2\, s_2\, t_3^2 + 16 \text{ similar terms}}{s_1^2\, s_2\, t_2 + s_1\, s_2\, s_3\, t_1 + 16 \text{ similar terms}},$$

with a similar expression for β_{AE}. Thus (3.1) serves as a compact shorthand for a lengthy and complicated formula.

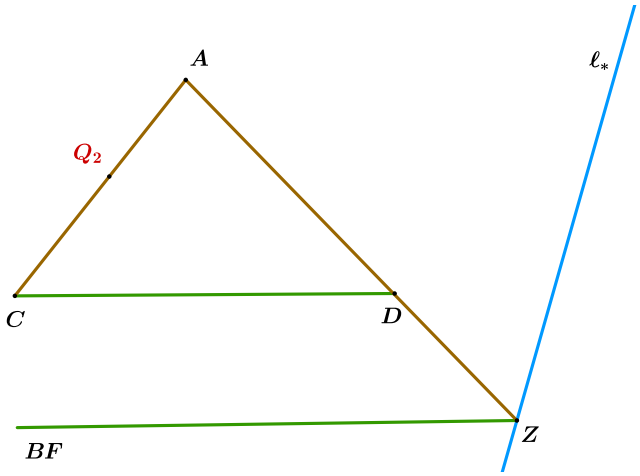

DIAGRAM 4. The double dependence of D on A

3.2. The second stage. We now use the fourth Pascal ℓ_*. Recall that a point on $\mathcal{K}$ is represented by the square of a linear form which is well-defined up to a scalar. Thus A comes from $a_{\mathbf{x}}$, where we are hoping to solve for a in terms of $s_1, t_1, \ldots, s_*, t_*$. There are two ways of expressing D in terms of A, and their comparison will lead to a set of equations for a.

Diagram 4 shows the geometric elements needed in the second step.

(1) Since the point Q_2 is on AC, the line AQ_2 is the same as AC. Now AQ_2 is represented by $(\mu_2, a_{\mathbf{x}}^2)_1 = a_{\mathbf{x}}\,(\mu_2, a_{\mathbf{x}})_1$. Hence C comes from the linear form $(\mu_2, a_{\mathbf{x}})_1$, and thus D comes from
$$\frac{\lambda_{CD}}{(\mu_2, a_{\mathbf{x}})_1}. \tag{3.2}$$

(2) The Pascal ℓ_* passes through $Z = AD \cap BF$, which implies that Z is represented by $(\ell_\star, \lambda_{BF})_1$. Hence AZ, which is the same as AD, is represented by
$$((\ell_*, \lambda_{BF})_1, a_{\mathbf{x}}^2)_1 = a_{\mathbf{x}}\,((\ell_*, \lambda_{BF})_1, a_{\mathbf{x}})_1.$$
Thus D also comes from
$$((\ell_*, \lambda_{BF})_1, a_{\mathbf{x}})_1. \tag{3.3}$$

The two linear forms in (3.2) and (3.3) must coincide up to a scalar. This gives the identity
$$\lambda_{CD} = \text{scalar} \times (\mu_2, a_{\mathbf{x}})_1 \times ((\ell_*, \lambda_{BF})_1, a_{\mathbf{x}})_1.$$
If we write $U = \lambda_{CD}$, $V = \mu_2$, $W = (\ell_*, \lambda_{BF})_1$, then, by Lemma 2.2, this is equivalent to $(U, (V, a_{\mathbf{x}})_1\,(W, a_{\mathbf{x}})_1)_1 = 0$.

The following transvectant identity allows us to rewrite this in such a way that we can extract a set of equations for a.

Proposition 3.2. For arbitrary quadratic forms U, V, W and linear form $a_{\mathbf{x}}$, we have an identity

$$(U, (V, a_{\mathbf{x}})_1 (W, a_{\mathbf{x}})_1)_1 = (M, a_{\mathbf{x}}^2)_2 + (N, a_{\mathbf{x}}^2)_1, \tag{3.4}$$

$$\text{where} \qquad M = \frac{1}{2}(U, W)_1 V + \frac{1}{2}(U, V)_1 W, \qquad N = -\frac{1}{2}(U, VW)_2 - \frac{1}{6} U (V, W)_2.$$

The proof will be given in section 4. The purpose of the identity is to 'package' the known quantities U, V, W into M and N, so as to separate them from the unknown quantity a.

3.3. Now write $M = (m_0, m_1, m_2, m_3, m_4)(x_1, x_2)^4$, and $N = (n_0, n_1, n_2)(x_1, x_2)^2$. The coefficients of U, V, W are rational functions of $s_1, \ldots, t_*$, hence so are all the m_i and n_i. The right-hand side of (3.4) can be expanded as $(r_0, r_1, r_2)(x_1, x_2)^2$, where each r_i is quadratic in a. Since this must vanish identically, we get three quadratic equations $r_0 = r_1 = r_2 = 0$ for a. A straightforward expansion shows that they can be written as

$$\begin{bmatrix} m_2 - n_1 & n_0 - 2m_1 & m_0 \\ 2m_3 - n_2 & -4m_2 & 2m_1 + n_0 \\ m_4 & -2m_3 - n_2 & m_2 + n_1 \end{bmatrix} \begin{bmatrix} 1 \\ a \\ a^2 \end{bmatrix} = 0.$$

Let $Z = (z_{ij})$ denote the 3×3 matrix on the left; e.g., $z_{12} = n_0 - 2m_1$. Now, for instance, we can use its first two rows to solve for a, which gives

$$a = -\frac{z_{11}z_{23} - z_{13}z_{21}}{z_{12}z_{23} - z_{13}z_{22}}.$$

This proves that a is a rational function of $s_1, \ldots, t_*$. Since $e_{\mathbf{x}}$ is a constant multiple of $\frac{\lambda_{AE}}{a_{\mathbf{x}}}$, the same follows for e. The Pascal ℓ_* passes through the points $CD \cap BE, AE \cap CF$ which respectively lie on the green chords CD, AE. Hence the same argument as in the second stage gives the result for b, c, d, f. This proves the main theorem, assuming Propositions 3.1 and 3.2. □

The passage $\{s_1, t_1, \ldots, s_*, t_*\} \Rightarrow \{a, \ldots, f\}$ goes through two complicated algebraic identities neither of which has any obvious geometric content. Thus our reconstruction is not 'synthetic' in the classical sense of the word. We do not know of any natural ruler-and-compass type construction which begins with the Pascals and ends with the sextuple. It would be interesting to find one.

3.4. The theme of this paper is related to the Galois (or monodromy) group of Pascal lines in the sense of [12]. We explain this in brief. Assume the base field to be **C**. Write

$$(T - a)(T - b) \ldots (T - f) = T^6 - \tau_1 T^5 + \tau_2 T^4 - \tau_3 T^3 + \tau_4 T^2 - \tau_5 T + \tau_6,$$

where $\tau_1, \ldots, \tau_6$ are the elementary symmetric functions in $a, \ldots, f$. Let $\mathcal{Z}$ denote the space of *unordered* six points on $\mathcal{K}$. In fact $\mathcal{Z}$ is birational to $\mathrm{Sym}^6\mathcal{K} \simeq \mathbf{P}^6$, and its field of rational functions may be identified with $\mathcal{F} = \mathbf{C}(\tau_1, \ldots, \tau_6)$. We have a 60-1 cover $\mathcal{Y} \longrightarrow \mathcal{Z}$, where the fibre over an unordered sextuple corresponds to its collection of 60 Pascals. If $\langle 1, s_i, t_i \rangle, 1 \leqslant i \leqslant 60$ are the line coordinates of the Pascals, then the field of rational functions of $\mathcal{Y}$ is $\mathcal{F}(s_1, t_1, \ldots, s_{60}, t_{60})$. However, the inclusion

$$\mathcal{F}(s_1, t_1, \ldots, s_{60}, t_{60}) \subseteq \mathbf{C}(a, \ldots, f) \tag{3.5}$$

is actually an equality by our main theorem. Hence we have the following:

Proposition 3.3. The Galois group $\mathrm{Gal}(\mathcal{Y}/\mathcal{Z}) \simeq \mathrm{Gal}(\mathbf{C}(a, \ldots, f)/\mathbf{C}(\tau_1, \ldots, \tau_6))$ is isomorphic to the symmetric group on six letters.

It should be clarified that this result cannot be considered original to this paper. The fact that (3.5) is an equality is already implicit in Pedoe's proof in [20], although it is not so stated there.

4. Transvectant identities

In this section we will prove Propositions 3.1 and 3.2. The proofs rely upon the graphical formalism[4] introduced in [2] and further developed in [1, §2]. We will give a brief introduction to this calculus in §4.2 below.

4.1. We will first rewrite Proposition 3.1 in more general and precise form. Consider six general linear forms $a_{\mathbf{x}} = a_1x_1 + a_2x_2$, $b_{\mathbf{x}} = b_1x_1 + b_2x_2$, …, $f_{\mathbf{x}} = f_1x_1 + f_2x_2$, where a letter such as 'a' stands for a pair of variables (a_1, a_2) instead of a single one. We will also use the classical bracket notation $(ab) = a_1b_2 - a_2b_1$ for 2×2 determinants, and similarly for (cd), (bf), etc.

Write $U = (b_{\mathbf{x}}c_{\mathbf{x}}, d_{\mathbf{x}}f_{\mathbf{x}})_1$, $V = (a_{\mathbf{x}}c_{\mathbf{x}}, d_{\mathbf{x}}e_{\mathbf{x}})_1$, $W = (a_{\mathbf{x}}b_{\mathbf{x}}, e_{\mathbf{x}}f_{\mathbf{x}})_1$, and $\psi(U, V, W) = 6(U, VW)_2 - U(V, W)_2$. Define

$$\mathcal{S} = (da)(fc)(eb) - (ce)(bd)(af). \tag{4.1}$$

Proposition 4.1. With notation as above, we have $\psi(U, V, W) = \Phi\ a_{\mathbf{x}}e_{\mathbf{x}}$, where $\Phi = \frac{3}{4}(cd)(bf)\ \mathcal{S}$.

[4] It has a close affinity to the classical symbolic calculus as practiced by the German school of invariant theorists in the nineteenth century (cf. [7, 11, 17]). Section 2 of [1] explains the precise correspondence between these two formalisms.

Remark 4.2. The expression $\mathcal{S}$ has the following invariance property. Let J denote the operation of making a simultaneous exchange of letters $a \leftrightarrow b, e \leftrightarrow f$. Now $\mathcal{S}$ remains invariant under the action of J, since the bracket factors $(da), (fc), (eb)$ are respectively taken to $(db), (ec), (fa)$ and conversely. Similarly, let K and L respectively denote the operations

$$b \leftrightarrow c, f \leftrightarrow d, \quad \text{and} \quad a \leftrightarrow e, b \leftrightarrow f, c \leftrightarrow d.$$

Then K also leaves $\mathcal{S}$ invariant, whereas L changes it to $-\mathcal{S}$. The subgroup generated by J, K and L inside the permutation group on letters $a, \ldots, f$, is isomorphic to $\mathfrak{S}_3 \times \mathbf{Z}_2$.

4.2. Graphical calculus. The graphical calculus we use in this article is a notational shorthand for complicated expressions obtained from contractions of tensors. By the latter we simply mean multidimensional arrays of numbers. Each picture appearing in the following calculations is nothing more than shorthand for an expanded formula which typically would look like $\sum_i \sum_j \sum_k \sum_l A_{ij} B_{kli} C_{ljk}$ (or rather much more involved similar expressions) if written in full. Thus the distinction between the picture and the expanded formula is analogous to the distinction between a high level programming language and assembly code in computer science. The graphical notation is compact, easy to read and numerically precise. When evaluating such diagrams, there is no "up to scale" ambiguity: every -1 or $\frac{1}{2}$ factor is meaningful and makes the difference between a correct and an erroneous equation. For a pair of variables such as $\mathbf{x} = (x_1, x_2)$, $a = (a_1, a_2)$, etc. we will use the graphical notation

$:= x_i$,


$:= a_i$ etc.

Note that each of these "blobs" has a "leg" coming out of it which carries an index with values in $\{1, 2\}$. By definition,

$:= \sum_{i=1}^{2} a_i x_i = a_{\mathbf{x}}$.

The rule of our graphical calculus is very simple. If a picture is obtained by an assembly of previously defined pieces like the a and x blobs, one takes the product of corresponding tensors, and for each pair of legs that have been glued one has to assign to it an index which is to be summed over the two-element set $\{1, 2\}$. Let $G(x_1, x_2)$ be a binary form of degree m. Then it can be written as

$$G(x_1, x_2) = \sum_{i_1, \ldots, i_m = 1}^{2} G_{i_1 \ldots i_m} \, x_{i_1} \cdots x_{i_m}$$

where the tensor $G_{i_1 \ldots i_m}$ is completely symmetric in its m indices. It can be recovered from the binary form by

$$G_{i_1 \ldots i_m} = \frac{1}{m!} \frac{\partial^m}{\partial x_{i_1} \cdots \partial x_{i_m}} G(x_1, x_2) \, .$$

We can define a new graphical piece or "G blob" by

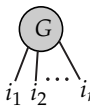

$$:= G_{i_1 \ldots i_m} \, .$$

By the same rule as before,

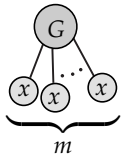

$$:= \sum_{i_1,\ldots,i_m=1}^{2} G_{i_1 \ldots i_m} x_{i_1} \cdots x_{i_m} \, .$$

Also needed are the Kronecker delta i —— j $:= \delta_{ij}$ and the ϵ arrow $i \longleftarrow j$ $:= \epsilon_{ij}$ where

$$(\epsilon_{ij})_{1 \leqslant i,j \leqslant 2} = \begin{pmatrix} 0 & 1 \\ -1 & 0 \end{pmatrix} \, .$$

Again, by the previous rule,

$$:= \sum_{i,j=1}^{2} a_i \epsilon_{ij} b_j = (ab) \, .$$

The Grassmann-Plücker relation for 2×2 determinants is the identity

$$(ab)(cd) = (ac)(bd) - (ad)(bc) \, .$$

If one applies to it the differential operator $\frac{\partial}{\partial a_i} \frac{\partial}{\partial b_j} \frac{\partial}{\partial c_k} \frac{\partial}{\partial d_l}$, then one obtains the equality

$$\epsilon_{ij} \epsilon_{kl} = \epsilon_{ik} \epsilon_{jl} - \epsilon_{il} \epsilon_{jk} \tag{4.2}$$

which is valid for any of the 2^4 value assignements for the indices i, j, k, l. This can be rewritten graphically as

(4.3)

When a picture is made of several connected components, then its evaluation is, by definition, the product of the evaluations of the connected components.

The transvectant in (2.1) can be written as

$$\begin{aligned}
(G,H)_r &= \frac{(m-r)!(n-r)!}{m!\, n!} \left\{ \left(\frac{\partial}{\partial x_1} \frac{\partial}{\partial y_2} - \frac{\partial}{\partial x_2} \frac{\partial}{\partial y_1} \right)^r G(\mathbf{x}) H(\mathbf{y}) \right\} \Big|_{\mathbf{y}:=\mathbf{x}} \\
&= \frac{(m-r)!(n-r)!}{m!\, n!} \left\{ \left(\sum_{i,j=1}^{2} \frac{\partial}{\partial x_i} \epsilon_{ij} \frac{\partial}{\partial y_j} \right)^r G(\mathbf{x}) H(\mathbf{y}) \right\} \Big|_{\mathbf{y}:=\mathbf{x}} \\
&= \sum_{i_1,\ldots,i_r=1}^{2} \; \sum_{j_1,\ldots,j_r=1}^{2} \; \sum_{k_1,\ldots,k_{m-r}=1}^{2} \; \sum_{l_1,\ldots,l_{n-r}=1}^{2} \epsilon_{i_1 j_1} \cdots \epsilon_{i_r j_r} \\
&\qquad G_{i_1 \ldots i_r k_1 \ldots k_{m-r}} \, H_{j_1 \ldots j_r l_1 \ldots l_{n-r}} \, x_{k_1} \cdots x_{k_{m-r}} x_{l_1} \cdots x_{l_{n-r}}
\end{aligned} \tag{4.4}$$

$=:$ 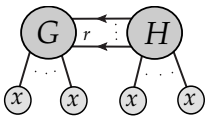

(4.5)

where the floating label r indicates the number of ϵ arrows between the G and H blobs. The number of x blobs hanging under the G blob is $m-r$ and that under the H blob is $n-r$. The symmetry of the G and H tensors was used in the derivation of the third line, whereas the last line is the definition of the corresponding picture via the same rule as before. The picture (4.5) is shorthand notation for the expanded formula (4.4). This picture is obtained by assembling: one G blob, one H blob, r epsilon arrows and $m+n-2r$ x blobs. The number of leg contractions is $2r+(m-r)+(n-r)$ which accounts for the $m+n$ indices which need to be summed over. There is a slight ambiguity in our rule regarding the correspondence between legs and the positions of indices for the tensor entries. A reader following a more strict interpretation of our rule would have written $G_{k_1\ldots k_{m-r}i_r\ldots i_1}$ instead of $G_{i_1\ldots i_r k_1\ldots k_{m-r}}$ in the third line. However, this does not affect the evaluation of the picture because of the complete symmetry of the G tensor/blob. Such a more strict handling of index labeling is needed for nonsymmetric tensors (see, e.g., the counterclockwise rule in [9, §4.1]). Another important remark is that the names of indices do not matter since they are dummy summation variables.

Suppose that the form H factorizes as $H=VW$, with V a binary form of degree p and W a binary form of degree q such that $p+q=n$. Then in general $H_{i_1\ldots i_n} \neq V_{i_1\ldots i_p}W_{i_{p+1}\ldots i_n}$, or graphically

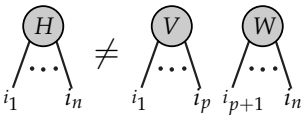

.

This motivates the introduction of another important piece for our graphical formalism: a particular tensor called a symmetrizer. Using Kronecker deltas and a sum over permutations $\sigma \in \mathfrak{S}_n$, let

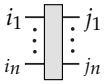

$:= \mathrm{Sym}_{i_1\ldots i_n, j_1\ldots j_n} := \dfrac{1}{n!}\displaystyle\sum_{\sigma\in\mathfrak{S}_n} \delta_{i_1 j_{\sigma(1)}}\cdots\delta_{i_n j_{\sigma(n)}}$.

For all permutations $\tau \in \mathfrak{S}_n$ and all index assignments $(i_1,\ldots,i_n,j_1,\ldots,j_n) \in \{1,2\}^{2n}$, one has the identity

$$\mathrm{Sym}_{i_1\ldots i_n, j_{\tau(1)}\ldots j_{\tau(n)}} = \mathrm{Sym}_{i_1\ldots i_n, j_1\ldots j_n} \,. \tag{4.6}$$

The new symmetrizer piece allows one to write the correct formula for the H tensor

$$H_{i_1\ldots i_n} = \sum_{j_1,\ldots,j_n=1}^{2} \mathrm{Sym}_{i_1\ldots i_n, j_1\ldots j_n} V_{j_1\ldots j_p} W_{j_{p+1}\ldots j_n} \tag{4.7}$$

or, graphically,

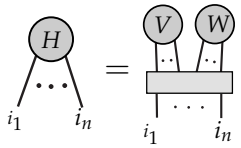

Substituting (4.7) in (4.4) and, with the strongest sense of urgency, converting the resulting expanded formula into graphical shorthand, we get

$(G, H)_r =$ 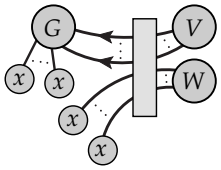 . (4.8)

The foregoing explanation should suffice in order to follow the graphical computations in this article. As additional help, we will also explicitly indicate the expanded formulae corresponding to some of the pictures in the beginning. However, we strongly recommend that the reader should also consult Section 2 of [1] (all the other sections can be safely ignored, since they pertain to an entirely different application of the graphical calculus).

Before concluding this section about the graphical formalism let us relate ours to that used by other authors. The BRL formalism by Blinn (see [4] and references therein) as well as Richter-Gebert and Lebmeir [22] is similar to ours. The main difference is that the BRL formalism adds arrows in order to distinguish legs or indices which correspond to vectors versus covectors. For instance, $i \longleftarrow j$ would denote δ_{ij} in BRL notations. The distinction of incoming versus outgoing legs does not matter for our bottom line which is the numerical evaluation of the expanded formula summarized by the picture. For the same reason, we do not raise or lower indices as is customary in the physics literature. Our arrows mean an ϵ tensor has been inserted between both ends. Another notable difference is that the BRL formalism, aiming for different goals than ours, does not use symmetrizers. The Cvitanović formalism [9] also uses arrows in order distinguish vectors from covectors. However, it makes extensive use of symmetrizers and antisymmetrizers: see for instance the beautiful proof of the Cayley-Hamilton Theorem in [9, §6.5] which inspired [18, Prop. 7.1] or that of the formula for the dimensions of GL_n representations [9, Appendix B.4]. The only other difference with our formalism is that we use grey shaded rectangles for symmetrizers instead of white ones in [9]. Finally, another treatment is that by Dolotin and Morozov [10] which uses two variants of the graphical calculus: one which uses arrows or orientations for the vector versus covector distinction and one which does not. The latter uses instead different colours (black and white) for the corresponding blobs/vertices and is thus closer to our formalism. This second version also uses a cross symbol or a white diamond for epsilon tensors.

4.3. We now resume the proof of Proposition 4.1.

Lemma 4.3. We have the more symmetric rewriting

$$\psi(U,V,W) = 3\left[(U,V)_2 W + (U,W)_2 V - (V,W)_2 U\right] .$$

Proof. Using the graphical formalism, we can write

$$(U,VW)_2 = \quad := \sum_{l_1,l_2=1}^{2} \sum_{i_1,\ldots,i_4=1}^{2} \sum_{j_1,\ldots,j_4=1}^{2}$$

$$U_{l_1 l_2} \epsilon_{l_1 i_1} \epsilon_{l_2 i_2} x_{i_3} x_{i_4} \mathrm{Sym}_{i_1 \ldots i_4, j_1 \ldots j_4} V_{j_1 j_2} W_{j_3 j_4} .$$

Note that the apparent asymmetry between V and W in the picture is not really there as can be seen from the identity (4.6) with the permutation $\tau = (13)(24)$ and a renaming of dummy summation indices. By expanding the sum over the permutation σ in the definition of the symmetrizer $\mathrm{Sym}_{i_1 \ldots i_4, j_1 \ldots j_4}$ (represented by the grey rectangle) one obtains

$$(U,VW)_2 = \frac{1}{4!}\left[4(U,V)_2 W + 4(U,W)_2 V + 16 \quad\right] . \tag{4.9}$$

Indeed, there are many equalities among the 24 terms generated by this expansion. They are consequences of the symmetries of the U, V, W matrices and renaming of indices. For example, the four permutations giving the $(U,V)_2 W$ contribution are the elements of the Klein four-group stabilizing the subset $\{1,2\} \subset \{1,2,3,4\}$.

We will use the notation

$$\{V \to U \leftarrow W\} := \quad .$$

Inserting the matrix identity $\epsilon\epsilon^{\mathrm{T}} = I$ between the W and x blobs, and using the Grassmann-Plücker relation (4.3) where indicated by the dotted line, we have

$$\{V \to U \leftarrow W\} = \quad = \quad - \quad .$$

In terms of nongraphical expanded formulas, the last equation simply says

$$\sum_{a,b,i,j,k,l,p,q=1}^{2} \epsilon_{ab} U_{ai} W_{bk} \epsilon_{ij} \epsilon_{kl} V_{jp} x_p \epsilon_{ql} x_q \;=$$

$$\sum_{a,b,i,j,k,l,p,q=1}^{2} \epsilon_{ab} U_{ai} W_{bk} \epsilon_{ik} \epsilon_{jl} V_{jp} x_p \epsilon_{ql} x_q \;- \sum_{a,b,i,j,k,l,p,q=1}^{2} \epsilon_{ab} U_{ai} W_{bk} \epsilon_{il} \epsilon_{jk} V_{jp} x_p \epsilon_{ql} x_q$$

as follows from (4.2).

As a result,

$$\{V \to U \leftarrow W\} + \{U \to W \leftarrow V\} = (U, W)_2 V \,. \tag{4.10}$$

Permuting U, V and W in the last identity gives three equations. They can be written in matrix form as

$$\begin{pmatrix} (V,W)_2 U \\ (U,W)_2 V \\ (U,V)_2 W \end{pmatrix} = \begin{pmatrix} 0 & 1 & 1 \\ 1 & 0 & 1 \\ 1 & 1 & 0 \end{pmatrix} \begin{pmatrix} \{V \to U \leftarrow W]\} \\ \{U \to V \leftarrow W\} \\ \{U \to W \leftarrow V\} \end{pmatrix} .$$

By inverting this matrix, we get

$$\{V \to U \leftarrow W\} = \frac{1}{2}\left[-(V,W)_2 U + (U,W)_2 V + (U,V)_2 W\right] \,. \tag{4.11}$$

After substituting back in (4.9) and simplifying, we get the required expression. □

The next lemma will be useful in the calculation of ψ.

Lemma 4.4. We have the transvectant identity

$$(\alpha_{\mathbf{x}}\beta_{\mathbf{x}}, \gamma_{\mathbf{x}}\delta_{\mathbf{x}})_1 = \frac{1}{2}(\alpha\gamma)\beta_{\mathbf{x}}\delta_{\mathbf{x}} + \frac{1}{2}(\beta\delta)\alpha_{\mathbf{x}}\gamma_{\mathbf{x}} \,. \tag{4.12}$$

Proof. Write

$(\alpha_{\mathbf{x}}\beta_{\mathbf{x}}, \gamma_{\mathbf{x}}\delta_{\mathbf{x}})_1 =$ 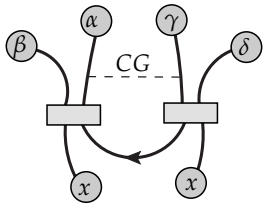

(4.13)

and apply the Clebsch-Gordan (CG) identity in [1, Eq. 2.9] at the place indicated by the dashed line. This gives

$(\alpha_{\mathbf{x}}\beta_{\mathbf{x}}, \gamma_{\mathbf{x}}\delta_{\mathbf{x}})_1 =$ 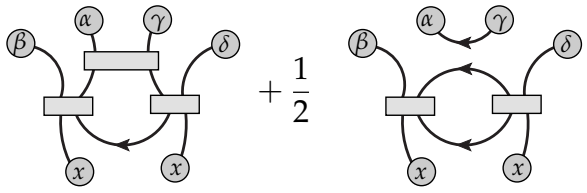

.

The weights 1 and $\frac{1}{2}$ come from the ratios of binomial coefficients in [1, Eq. 2.9] in the $(m, n) = (1, 1)$ case where m, n refer to the notation in [1, Eq. 2.9]. In expanded form, this identity simply is $\delta_{ik}\delta_{jl} = \mathrm{Sym}_{ij,kl} + \frac{1}{2}\epsilon_{ij}\epsilon_{kl}$ which follows from (4.2), or rather, its dualized

version $\epsilon_{ij}\epsilon_{kl} = \delta_{ik}\delta_{jl} - \delta_{il}\delta_{jk}$. After expanding the symmetrizers, we get

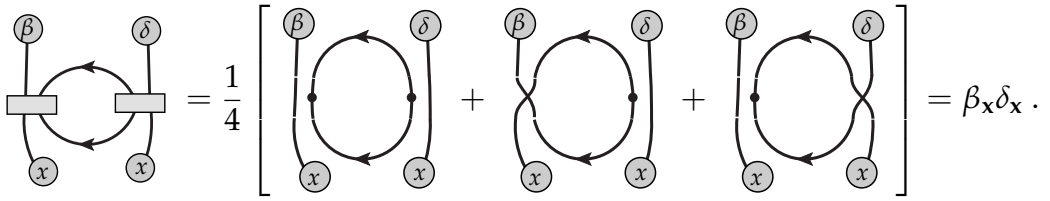

Note that we omited the fourth diagram with two crossings, since it contains the factor $(\mathbf{xx}) = 0$. By applying the same CG identity to the β and δ strands, we get

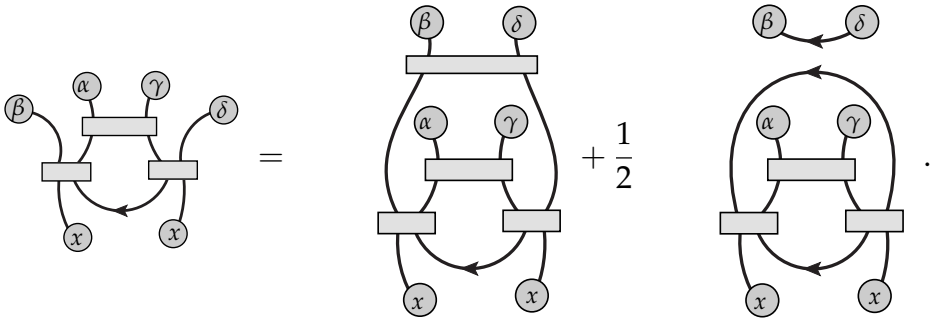

The second diagram can be computed by expanding the bottom two symmetrizers as above, which gives the expression $(\beta\delta)\alpha_{\mathbf{x}}\gamma_{\mathbf{x}}$. We claim that the first diagram vanishes. Indeed, due to the presence of the top two symmetrizers, if we move the bottom two symmetrizers so that they exchange places, then the diagram becomes its own negative since this move reverses the orientation of the bottom arrow. Now we get the required identity by substituting back in the last equation for $(\alpha_{\mathbf{x}}\beta_{\mathbf{x}}, \gamma_{\mathbf{x}}\delta_{\mathbf{x}})_1$. □

Remark 4.5. The left-hand side of (4.12) corresponds to a pair partition $\{\{\alpha,\beta\},\{\gamma,\delta\}\}$. We implicitly chose the 'transverse' partition $\{\{\alpha,\gamma\},\{\beta,\delta\}\}$ for the right-hand side. However, we could have instead chosen $\{\{\alpha,\delta\},\{\beta,\gamma\}\}$, which would give the equally valid identity

$$(\alpha_{\mathbf{x}}\beta_{\mathbf{x}}, \gamma_{\mathbf{x}}\delta_{\mathbf{x}})_1 = \frac{1}{2}(\alpha\delta)\beta_{\mathbf{x}}\gamma_{\mathbf{x}} + \frac{1}{2}(\beta\gamma)\alpha_{\mathbf{x}}\delta_{\mathbf{x}}.$$

If we average the last equality with (4.12), the net result is the 'naive' four-term expansion of the transvectant as in [11, §44 and §49 (vii)] or as produced by expanding the two symmetrizers in (4.13). If one were to use the four-term expansion for a brute-force bracket monomial computation of ψ, this would generate $4^3 \times 2 \times 3 = 384$ terms. (The factors of 4 come from the calculation of U, V and W. The factor of 2 comes from the computation of second transvectants, and finally there are 3 terms such as $(U, V)_2 W$.) Hence the previous lemma is essential in organizing the calculation of ψ and reducing its complexity.

4.4. By Lemma 4.4, $U = \frac{1}{2}(cd)b_{\mathbf{x}}f_{\mathbf{x}} + \frac{1}{2}(bf)c_{\mathbf{x}}d_{\mathbf{x}}$ and $V = \frac{1}{2}(cd)a_{\mathbf{x}}e_{\mathbf{x}} + \frac{1}{2}(ae)c_{\mathbf{x}}d_{\mathbf{x}}$. Using the bilinearity of the second transvectant, we have

$$\begin{aligned}4(U,V)_2 =&(cd)^2(b_{\mathbf{x}}f_{\mathbf{x}}, a_{\mathbf{x}}e_{\mathbf{x}})_2 + (cd)(ae)(b_{\mathbf{x}}f_{\mathbf{x}}, c_{\mathbf{x}}d_{\mathbf{x}})_2 + \\ &(bf)(cd)(c_{\mathbf{x}}d_{\mathbf{x}}, a_{\mathbf{x}}e_{\mathbf{x}})_2 + (bf)(ae)(c_{\mathbf{x}}d_{\mathbf{x}}, c_{\mathbf{x}}d_{\mathbf{x}})_2.\end{aligned}$$

Now

$$(c_{\mathbf{x}}d_{\mathbf{x}}, c_{\mathbf{x}}d_{\mathbf{x}})_2 = \quad$$ 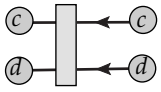

$$= -\frac{1}{2}(cd)^2$$

and thus $(U,V)_2 = \frac{1}{4}(cd)\ \mathcal{S}'$, where

$$\mathcal{S}' = (cd)(b_xf_x, a_xe_x)_2 + (ae)(b_xf_x, c_xd_x)_2 + (bf)(c_xd_x, a_xe_x)_2 - \frac{1}{2}(ae)(bf)(cd)\ .$$

We will show later that $\mathcal{S}'$ is in fact equal to the $\mathcal{S}$ of (4.1). Since second transvectants are symmetric bilinear forms, the previously mentioned symmetries of $\mathcal{S}$ are particularly evident in the last equation.

By Lemma 4.4, we have $W = \frac{1}{2}(ae)b_{\mathbf{x}}f_{\mathbf{x}} + \frac{1}{2}(bf)a_{\mathbf{x}}e_{\mathbf{x}}$ and this results in

$$(U,V)_2W = \frac{1}{8}\mathcal{S}' \times \{(cd)(ae)b_{\mathbf{x}}f_{\mathbf{x}} + (cd)(bf)a_{\mathbf{x}}e_{\mathbf{x}}\}\ . \tag{4.14}$$

The exchange of letters $b \leftrightarrow c, d \leftrightarrow f$ brings about an exchange of V and W. Applying this to (4.14) gives

$$(U,W)_2V = \frac{1}{8}\mathcal{S}' \times \{(bf)(ae)c_{\mathbf{x}}d_{\mathbf{x}} + (bf)(cd)a_{\mathbf{x}}e_{\mathbf{x}}\}\ . \tag{4.15}$$

Likewise, the exchange $a \leftrightarrow c, d \leftrightarrow e$ exchanges U and W. Applying this to (4.14) gives

$$(W,V)_2U = \frac{1}{8}\mathcal{S}' \times \{(ae)(cd)b_{\mathbf{x}}f_{\mathbf{x}} + (ae)(bf)c_{\mathbf{x}}d_{\mathbf{x}}\}\ . \tag{4.16}$$

Now substitute (4.14), (4.15), and (4.16) in the result of Lemma 4.3 and simplify. This gives the required formula for ψ.

4.5. We now proceed with the simplification of $\mathcal{S}'$. By expanding the symmetrizers implicit in the three second transvectants, we get

$$\begin{aligned}2\mathcal{S}' =&(cd)(ba)(fe) + (cd)(be)(fa) + (ae)(bc)(fd) + \\ &(ae)(bd)(fc) + (bf)(ca)(de) + (bf)(ce)(da) - (ae)(bf)(cd).\end{aligned}$$

Now insert the GP relation $(ba)(fe) = (bf)(ae) - (be)(af)$ in the first term, and similarly the relations $(bc)(fd) = (bf)(cd) - (bd)(cf)$, $(ca)(de) = (cd)(ae) - (ce)(ad)$ respectively

in the third and the fifth term. After an expansion, cancellation and a division by 2, we get

$$\mathcal{S}' = (cd)(be)(fa) + (ae)(bd)(fc) + (bf)(ce)(da) + (ae)(bf)(cd).$$

Now insert the GP relations $(cd)(be) = (cb)(de) - (ce)(db)$, $(bf)(ce) = (bc)(fe) - (be)(fc)$ respectively in the first and the third term, to get

$$\mathcal{S}' = \underbrace{-(ce)(db)(fa) - (be)(fc)(da)}_{\mathcal{S}} + \mathcal{T},$$

where $\mathcal{T} = (cb)(de)(fa) + (ae)(bd)(fc) + (bc)(fe)(da) + (ae)(bf)(cd)$. We only need to verify that $\mathcal{T}$ is identically zero, which would imply $\mathcal{S}' = \mathcal{S}$. To this end, insert the GP relations $(de)(fa) = (df)(ea) - (da)(ef)$, $(bd)(fc) = (bf)(dc) - (bc)(df)$ respectively in the first and second term of $\mathcal{T}$. The six resulting terms cancel in pairs, and thus $\mathcal{T} = 0$. This completes the proof of Proposition 3.1. □

4.6. The invariant $\mathcal{S}$ has played an important role in the proof. The following proposition gives another notable property of this invariant.

Proposition 4.6. The polynomial $\mathcal{S}$ and the simpler expression $(ae)(bf)(cd)$ form a basis of the vector space of multilinear SL_2-invariants of $a, b, \ldots, f$ which satisfy the $\mathfrak{S}_3 \times \mathbf{Z}_2$ symmetry mentioned in Remark 4.2.

We omit the proof, since this result is not essential for our main theorem. It is a straightforward application of the First Fundamental Theorem of classical invariant theory and Kempe's Circular Straightening Theorem (see, e.g, [13, Prop. 2.6] or [17, Lemma 6.2]).

Remark 4.7. There is a simple combinatorial recipe for finding the two bracket monomials appearing in $\mathcal{S}$. Draw the oriented graph on six vertices given by the edges $a \leftarrow e$, $b \leftarrow f$, $c \leftarrow d$, which correspond to the three quadratics used to build U, V and W. Now ask: how can one add three more directed edges in order to form a *properly oriented* 6-cycle? The two possible answers give the two required bracket monomials. More precisely, if we take the convention that a bracket (uv) corresponds to an oriented edge $u \leftarrow v$, and if one sums over the two answers then one gets $(da)(fc)(eb) + (fa)(db)(ec) = \mathcal{S}$. Interestingly, if one takes the difference $\mathcal{J} = (da)(fc)(eb) - (fa)(db)(ec)$ then one would obtain the Wronskian invariant considered by Joubert [14, p. 1026] which, e.g., features in the recent work [16, p. 246] and [5, p. 170].

4.7. Proof of Proposition 3.2. Recall that U, V, W are now arbitrary quadratics, and $a_{\mathbf{x}}$ is a linear form. By expanding the symmetrizer, we have

$$(U,(V,a_{\mathbf{x}})_1(W,a_{\mathbf{x}})_1)_1 = \quad = \frac{1}{2}G_{\mathrm{v}} + \frac{1}{2}G_{\mathrm{w}}$$

with

$G_{\mathrm{v}} =$ and $G_{\mathrm{w}} =$.

We will compute G_{v} and deduce the analogous formula for G_{w} by exchanging V and W. One can rewrite

$G_{\mathrm{v}} =$

and apply the CG identity [1, Eq. 2.9] between the bottom two symmetrizers. This results in $G_{\mathrm{v}} = G_{\mathrm{v}0} + G_{\mathrm{v}1} + \frac{1}{3}G_{\mathrm{v}2}$ with

$G_{\mathrm{v}0} =$, $G_{\mathrm{v}1} =$, and $G_{\mathrm{v}2} =$.

It is the $(m,n) = (2,2)$ case of [1, Eq. 2.9] which has been use here. In nongraphical expanded form, it is the statement that $\forall (i,j,k,l,a,b,c,d) \in \{1,2\}^8$,

$$\mathrm{Sym}_{ij,kl}\,\mathrm{Sym}_{ab,cd} \;=\; \mathrm{Sym}_{ijab,klcd}$$
$$+ \sum_{p_1,p_2=1}^{2}\sum_{q_1,q_2=1}^{2}\sum_{r_1,r_2=1}^{2}\sum_{s_1,s_2=1}^{2} \mathrm{Sym}_{ij,r_1p_1}\mathrm{Sym}_{ab,q_1s_1}\epsilon_{p_1q_1}\mathrm{Sym}_{r_1s_1,r_2s_2}\epsilon_{p_2q_2}\mathrm{Sym}_{r_2p_2,kl}\mathrm{Sym}_{q_2s_2,cd}$$
$$+\frac{1}{3}\sum_{p_1,p_2=1}^{2}\sum_{q_1,q_2=1}^{2}\sum_{r_1,r_2=1}^{2}\sum_{s_1,s_2=1}^{2} \mathrm{Sym}_{ij,r_1p_1}\mathrm{Sym}_{ab,q_1s_1}\epsilon_{p_1q_1}\epsilon_{r_1s_1}\epsilon_{r_2s_2}\epsilon_{p_2q_2}\mathrm{Sym}_{r_2p_2,kl}\mathrm{Sym}_{q_2s_2,cd}\,.$$

It can be proved by the expansion of symmetrizers and repeated use of the dualized GP relation, but the computation is tedious. The diligent reader may prefer to consult the

complete account given in [1, §2] of the beautiful original proof due to Paul Gordan and Alfred Clebsch for general formats (m, n).

Having the big symmetrizer eat up the smaller ones, we can write

$G_{\mathrm{v}0} =$ 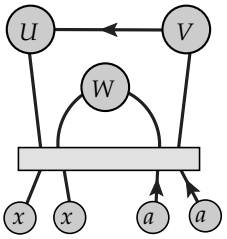 $= \left((U,V)_1 W, a_{\mathbf{x}}^2\right)_2 .$

Passing the bottom arrows through the right symmetrizer and using idempotence, we get

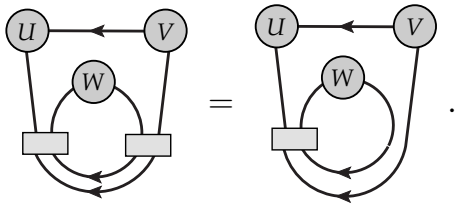

Now expand the symmetrizer and ignore the vanishing term with the W self-loop. This gives

$\frac{1}{2} =$ 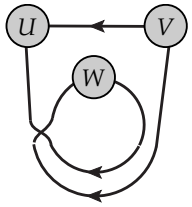 $= \frac{1}{2}$ 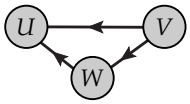 .

Note that, by the antisymmetry of the ϵ matrix, the last graph changes sign if one exchanges V and W. Therefore $G_{\mathrm{v}2} + G_{\mathrm{w}2} = 0$ where $G_{\mathrm{w}2}$ is the expression analogous to $G_{\mathrm{v}2}$ with V and W exchanged.

Now remove the redundant $\mathbf{x}$-symmetrizer and pass the arrows through the symmetrizer on the bottom right of the previous diagram for $G_{\mathrm{v}1}$. Then we have

$G_{\mathrm{v}1} = -$ 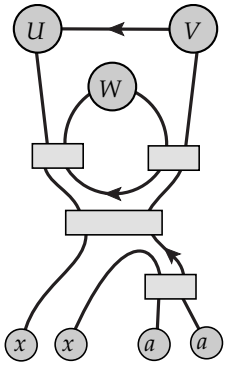 $= -(H_{\mathrm{v}}, a_{\mathbf{x}}^2)_1$ with $H_{\mathrm{v}} =$ 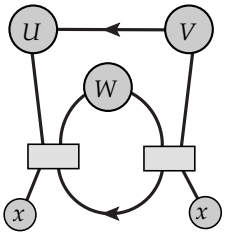

via a similar reasoning to that which led to (4.8). If we go through the same manipulations for G_{w} and add its contribution to that of G_{v}, then we get the required expression for M

together with

$$N = -\frac{1}{2}H_{\mathrm{v}} - \frac{1}{2}H_{\mathrm{w}}.$$

Here H_{w} is the expression similar to H_{v}, with V and W interchanged. Expanding the two symmetrizers and dropping the zero term with the W self-loop, we get

$H_{\mathrm{v}} = \frac{1}{4}$ 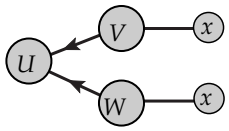 $+\frac{1}{4}$ 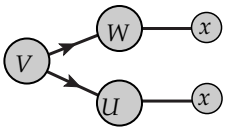 $+\frac{1}{4}$ 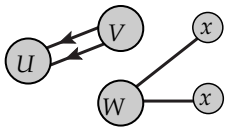 .

By identity (4.10), the sum of the first two terms is equal to the last, and thus

$$H_{\mathrm{v}} = \frac{1}{2}(U, V)_2 W\,. \tag{4.17}$$

We have seen in (4.9) that

$$(U, VW)_2 = \frac{1}{6}(U, V)_2 W + \frac{1}{6}(U, W)_2 V + \frac{2}{3}\{V \to U \leftarrow W\}\,.$$

Inserting (4.11) in the last equation, we get

$$(U, VW)_2 = \frac{1}{2}(U, V)_2 W + \frac{1}{2}(U, W)_2 V - \frac{1}{3}(V, W)_2 U\,.$$

By (4.17) and the analogous expression for H_{w}, we obtain

$$(U, VW)_2 = -2N - \frac{1}{3}(V, W)_2 U,$$

which gives the required expression for N. This completes the proof of Proposition 3.2. □

REFERENCES

[1] A. Abdesselam. On the volume conjecture for classical spin networks. *J. Knot Theory Ramifications*, vol. 21, no. 3, 1250022, 62 pp., 2012.

[2] A. Abdesselam and J. Chipalkatti. Brill-Gordan loci, transvectants and an analogue of the Foulkes conjecture. *Adv. Math.*, vol. 208, no. 2, pp. 491–520, 2007.

[3] H. F. Baker. *Principles of Geometry, vol. II.* Cambridge University Press, 1923.

[4] J. F. Blinn. Lines in space, part 8: line(s) through four lines. *IEEE Comput. Graph. Appl.*, vol. 24, no. 5, pp. 100–106, 2004.

[5] A.-M. Castravet and J. Tevelev. Hypertrees, projections, and moduli of stable rational curves. *J. Reine Angew. Math.*, vol. 675, pp. 121–180, 2013.

[6] J. Chipalkatti. On the coincidences of Pascal lines. *Forum Geometricorum*, vol. 16, pp. 1–21, 2016.

[7] A. Clebsch. *Theorie der Binären Algebraischen Formen.* B. G. Teubner, Leipzig, 1872.

[8] J. Conway and A. Ryba. The Pascal mysticum demystified. *Math. Intelligencer*, vol. 34, no. 3, pp. 4–8, 2012.

[9] P. Cvitanović. *Group Theory. Birdtracks, Lie's, and Exceptional Groups.* Princeton University Press, Princeton, NJ, 2008.

[10] V. Dolotin and A. Morozov. *Introduction to Non-Linear Algebra.* World Scientific Publishing Co. Pte. Ltd., Hackensack, NJ, 2007.

[11] J. H. Grace and A. Young. *The Algebra of Invariants.* Reprinted by Chelsea Publishing Co., New York, 1962.

[12] J. Harris. Galois groups of enumerative problems. *Duke Math. J.*, vol. 46, no. 4, pp. 685–724, 1979.

[13] B. Howard, J. Millson, A. Snowden and R. Vakil. The equations for the moduli space of n points on the line. *Duke Math. J.*, vol. 146, no. 2, pp. 175–226, 2009.

[14] Fr. Joubert. Sur l'équation du sixième degré. *C. R. Acad. Sci. Paris*, vol. 64, pp. 1025–1029, 1867.

[15] L. Kadison and M. T. Kromann. *Projective Geometry and Modern Algebra.* Birkhäuser, Boston, 1996.

[16] H. Kraft. A result of Hermite and equations of degree 5 and 6. *J. Algebra*, vol. 297, no. 1, pp. 234–253, 2006.

[17] J. P. S. Kung and G.-C. Rota. The invariant theory of binary forms. *Bull. American Math. Soc. (N.S.)*, vol. 10, no. 1, pp. 27–85, 1984.

[18] V. Lafforgue. Chtoucas pour les groupes réductifs et paramétrisation de Langlands globale. arXiv preprint arXiv:1209.5352[math.AG], 2012.

[19] P. Olver. *Classical Invariant Theory*. London Mathematical Society Student Texts. Cambridge University Press, 1999.

[20] D. Pedoe. How many Pascal lines has a sixpoint? *The Mathematical Gazette*, vol. 25, no. 264, pp. 110–111, 1941.

[21] D. Pedoe. *Geometry, A Comprehensive Course*. Reprinted by Dover Publications, New York, 1988.

[22] J. Richter-Gebert and P. Lebmeir. Diagrams, tensors and geometric reasoning. *Discrete Comput. Geom.*, vol. 42, no. 2, pp. 305–334, 2009.

[23] G. Salmon. *A Treatise on Conic Sections.* Reprint of the 6th ed. by Chelsea Publishing Co., New York, 2005.

[24] P. Schreck, P. Mathis, V. Marinković and P. Janičić. Wernick's list: a final update. *Forum Geometricorum*, vol. 16, pp. 69–80, 2016.

[25] A. Seidenberg. *Lectures in Projective Geometry*. D. Van Nostrand Company, New York, 1962.

[26] W. Wernick. Triangle constructions with three located points. *Math. Mag.*, vol. 55, no. 4, pp. 227–230, 1982.

—

Abdelmalek Abdesselam
Department of Mathematics,
University of Virginia,
P. O. Box 400137,
Charlottesville, VA 22904-4137,
USA.
malek@virginia.edu

Jaydeep Chipalkatti
Department of Mathematics,
Machray Hall,
University of Manitoba,
Winnipeg, MB R3T 2N2,
Canada.
jaydeep.chipalkatti@umanitoba.ca